Master's thesis
Astrophysical Sciences

Supermassive black holes and the cosmological formation of massive early-type galaxies (title not final)

Atte Keitaanranta

June 16, 2021

Supervisor(s): Prof. Peter Johansson
M.Sc. Matias Mannerkoski

Censor(s): Prof. Peter Johansson

UNIVERSITY OF HELSINKI
Department of Physics
PL 64 (Gustaf Hällströmin katu 2)
00014 University of Helsinki

HELSINGIN YLIOPISTO — HELSINGFORS UNIVERSITET — UNIVERSITY OF HELSINKI

Tiedekunta — Fakultet — Faculty	Koulutusohjelma — Utbildningsprogram — Education programme
Faculty of Science	Department of Physics

Tekijä — Författare — Author

Atte Keitaanranta

Työn nimi — Arbetets titel — Title

Supermassive black holes and the cosmological formation of massive early-type galaxies (title not final)

Opintosuunta — Studieinriktning — Study track

Astrophysical Sciences

Työn laji — Arbetets art — Level	Aika — Datum — Month and year	Sivumäärä — Sidoantal — Number of pages
Master's thesis	June 16, 2021	0 pages

Tiivistelmä — Referat — Abstract

Abstract goes here.

Avainsanat — Nyckelord — Keywords

Your keywords here

Säilytyspaikka — Förvaringsställe — Where deposited

Muita tietoja — övriga uppgifter — Additional information

Contents

1. Introduction

1.1 Information about galaxies, shortly

1.2 Aim of the thesis

2. Background

2.1 Cosmology

2.1.1 Hubble parameter, Friedmann equations and so on

2.1.2 Cosmological perturbations

2.2 Early-type galaxies

2.2.1 Types of ellipticals

2.2.2 Photometric and kinematic profiles

2.3 Feedback processes

3. GADGET-3 and KETJU

- Haven't really thought about the contents of this chapter yet

3.1 Overview of GADGET-3

3.2 Smoothed Particle Hydrodynamics

3.3 Gas cooling?

3.4 Feedback?

3.5 KETJU

4. Creating initial conditions for the cosmological simulations

This chapter focuses on the methods used to create the necessary configuration files for the high resolution cosmological simulations. First, we discuss the so-called 'zoom-in' method, which allows us to have spatially large simulation boxes with high resolution regions. After this, we discuss the code MUSIC (MUlti-Scale initial conditions), which used to create a spatial volume with highly accurate velocity and density perturbations, with the root-mean square (RMS) relative error being of the order 10^{-4} Hahn & Abel (2011). The created initial conditions (ICs) file is used for the performed GADGET-3 simulations. As the runs performed with GADGET-3 are the main focus of this thesis, the section for MUSIC is not as in-depth as the GADGET-3 discussion in chapter 3. The last part of this chaper focuses on the setup of the cosmological setup of the simulations, and on the preliminary low resolution run needed for the higher resolution simulations.

4.1 Zoom-in technique

To study galaxy formation and evolution in a proper cosmological context, our simulation box must have a large volume. To resolve the gravitational effects of a smaller scale structure, it is also required to have a high resolution, i.e. a large amount of particles with relatively low mass. Having a sufficient resolution on the whole simulation volume would result in a unreasonably large computational workload. Thus it is more sensible to implement a method, which has a high resolution in a single region of interest, surrounded by a large volume with a smaller resolution. This nowadays so-called 'zoom-in' technique has been in use for multiple decades. One of the first simulations with a region of interest surrounded by low resolution background was performed by Navarro & White (1994), and later implementations have been used by e.g. Power et al. (2003) and Marinacci et al. (2014). Modern

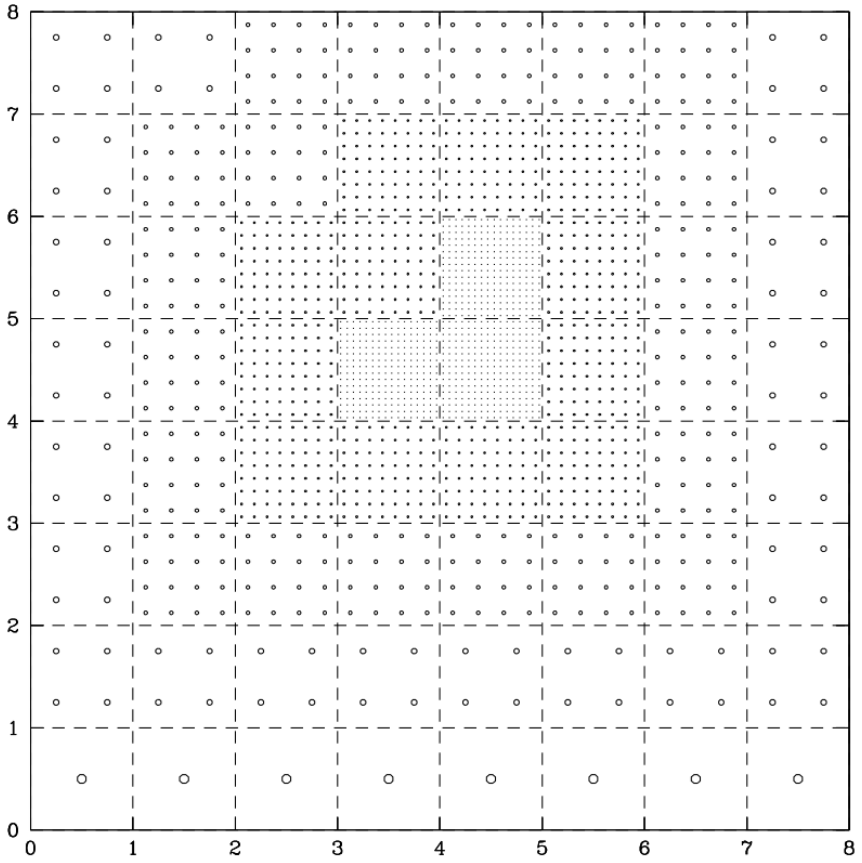

Figure 4.1: An example of a multiple scale mesh grid (Klypin et al., 2001). THIS CAPTION IS NOT FINISHED

implementations, such as the one used in this thesis, use zoom regions with multiple levels of smaller scale particles, as shown in Figure 4.1.

To locate the regions of intetrest, we need to first perform a computationally light simulation without a high resolution volume (discussed in SECTION REFERENCE HERE), and then choose the zoom-in region and perform the simulation again. The initial conditions (ICs) must also portray a realistic case, i.e. the fluctuations at a very high redshift must match the expected structure from theory. Fortunately, we can use a single program to create good ICs, with zoom-in box included.

4.2 Music

NOTE: some things might be mentioned without good explanations (like the power spectrum and two-point correlation), and I plan to explain them in chapter 2.

4.2.1 Overview

MUSIC (MUlti-Scale Initial Conditions) is a code by Navarro & White (1994), which can be used to create the ICs for GADGET-3 simulations. The program creates a simulation volume, with velocity and particle displacements calculated using a power spectrum and two-point correlation given as input. To take fluctuations of smaller scales into account, the program is also able to create a high resolution zoom-in region for the Ics. The zoom-in region can have multiple levels of refinement, with each cell divided to eight children, as shown in Figure 4.2.

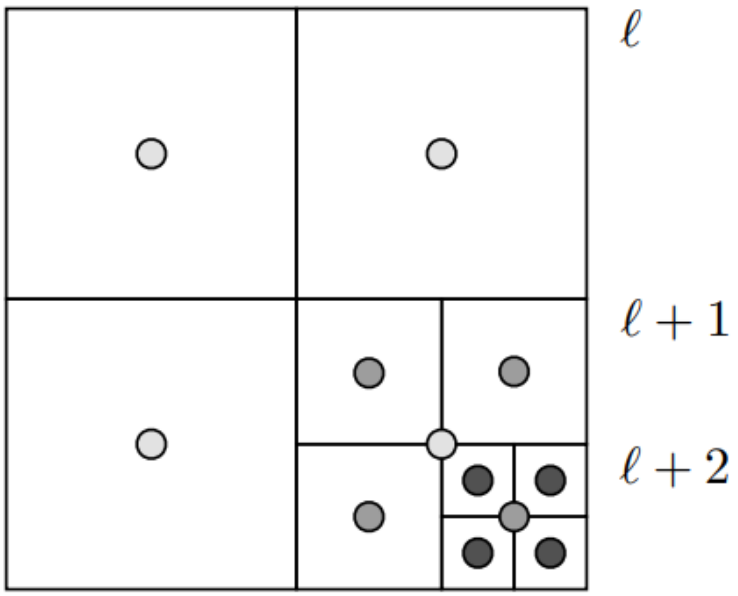

Figure 4.2: A two dimensional example layout of multiple scale nested grid (Hahn & Abel, 2011). The figure shows parent cells on level ℓ, and children cells on two higher levels. The center of the children cells is not in the same position as the center of the parent cell. NOTE: this figure might make fig 4.1 unnecessary (maybe change it to show just one level of zoom?). Maybe move this to the section where the cration of multiple refinement levels is discussed?

The algorithm is is not first of its kind. MUSIC extends the prior work, e.g. the GRAFIC-2 code made by Bertschinger (2001), which also produces ICs with multiple levels of resolution. The most significant upgrade of MUSIC compared to GRAFIC-2 is the way the trasfer function is used to calculate the density perturbations (discussed in 4.2.2).

The initial conditions produced by the code best describe the real conditions when the redshift of the produced ICs lie on the linear perturbation regime. If the initial redshift z_i of the ICs is set to be too large (i.e. on the non-linear regime), the

formation of the first haloes occurs at unrealistically late times and the formation of high-mass haloes is suppressed (e.g. Reed et al. (2013)). Still, MUSIC gives relatively accurate ICs even at the mildly non-linear regime of $z_i \sim 20$, (Hahn & Abel, 2011).

4.2.2 Generation of the density field

For the generation of particle velocities and locations, MUSIC first needs to create a density field, described by and over-density field $\delta(\mathbf{r})$. Using an a Power spectrum $P(k)$ given as input, this field can be described completely, as the power spectrum of the field is

$$P(k) \equiv \langle \tilde{\delta}(\mathbf{k}) \tilde{\delta}^*(\mathbf{k}) \rangle, \tag{4.1}$$

where * denotes the complex conjugate, and $\tilde{\delta}(\mathbf{k})$ represents the Fourier transform of the over-density field. The transfer function $T(k)$ can also be used to express the power spectrum, defined as

$$P(k) = \alpha k^{n_s} T^2(k), \tag{4.2}$$

where α is a normalization constant and n_s is the spectral index. The value of the spectral index is given to MUSIC in the configuration file, while α is evaluated in using another, observable constant.

One way to normalize the spectrum estimate the amplitude of the via the observable variance of the galaxy distribution σ^2 at a distance R. As shown in e.g. (SOURCE: Mo, Bosch, White) , the predicted variance is defined as

$$\sigma^2(R) = \frac{1}{2\pi^2} \int P(k) \tilde{W}^2(k) k^2 \mathrm{d}k, \tag{4.3}$$

where $\tilde{W}(k)$ is defined as the Fourier transform of a top-hat window function $W(r)$:

$$W(r) = \begin{cases} \frac{3}{4\pi R^3}, & r \leq R \\ 0, & r > R \end{cases} \tag{4.4}$$

The Fourier transform of this function is

$$\tilde{W}(k) = \frac{3}{(kR)^3} \left(\sin(kR) - kR \cos(kR) \right). \tag{4.5}$$

The distance where the variance is usually measured is $R = 8\,\mathrm{Mpc/h}$. At this distance, $\sigma(8\,\mathrm{Mpc/h}) \equiv \sigma_8$ is valued close to unity. σ_8 is also the value MUSIC takes as input to normalize the power spectrum.

- how input power spectrum is used
- The real-space transfer function
- Gaussian white noise
- Multiple levels of grids
- Density fields calculated 'bottom-up' (finest level constraints coarser level)
- Skip/don't go into detail: convolution kernels, noise convolution

4.2.3 Particle displacements and velocity fields

- Lagrangian perturbation theory (might be explained already in earlier chapters?)
- Poisson's equation and its multi-grid solution
- MUSIC uses hybrid Poisson solver
- Differences between baryons and DM

4.2.4 Creating IC files

- Step by step explanation of creating the IC file with a zoom-in region

4.3 GADGET-3 setup for the zoom-in -simulations

4.3.1 Cosmological setup

4.3.2 Low-resolution run

4.3.3 Choosing the zoom-in regions

- FoF -algorithm
- Conditions of the chosen halos
- Figure showing the zoom-in regions from the low res run

4.3.4 Initial conditions

- Information from GADGET3 config files

h_0	Ω_m	Ω_b	Ω_Λ	σ_8	ρ_{crit}
70.3	0.276	0.045	0.724	0.811	$9.28 \times 10^{-27}\ \mathrm{kg/m^3}$

Table 4.1: Cosmological parameters used for the simulations. If a simulation doesn't include baryons, the dark matter density parameter Ω_{DM} is equal to the matter density parameter Ω_{m}. If baryons are included, $\Omega_{\mathrm{DM}} = \Omega_{\mathrm{m}} - \Omega_{\mathrm{b}}$.

5. Cosmological GADGET-3 simulations

5.1 Computational load of the simulations

- Quick overview: CPUs used, time elapsed, where simulations were run

5.2 Locating galaxy centers: the shrinking sphere -method

5.3 Properties of the galaxies

Simulation	r_{vir} (kpc)	M_* ($M_\odot$)	M_{V} (mag)	$M_{*,\mathrm{gal}}/M_{\mathrm{vir}}$	M_{bh} ($M_\odot$)
Med res, A	517	3.98×10^{11}	-22.4	0.025	5.82×10^9
Med res, B	574	5.16×10^{11}	-22.7	0.024	6.23×10^9
Med res, C	400	2.56×10^{11}	-22.0	0.035	3.96×10^9
High res, A	526	5.31×10^{11}	-22.6	0.032	3.64×10^9
High res, B	578	6.38×10^{11}	-22.8	0.029	4.54×10^9
High res, C	400	3.46×10^{11}	-22.2	0.047	2.80×10^9

Table 5.1: Properties of the zoomed-in galaxies at redshift $z = 0$.

5.3.1 Rotation curves

- Med res galaxy A simulation is performed with single precision, I'm currently doing the simulation in double precision
- Rotation curves do not have the same limits on the y-axis

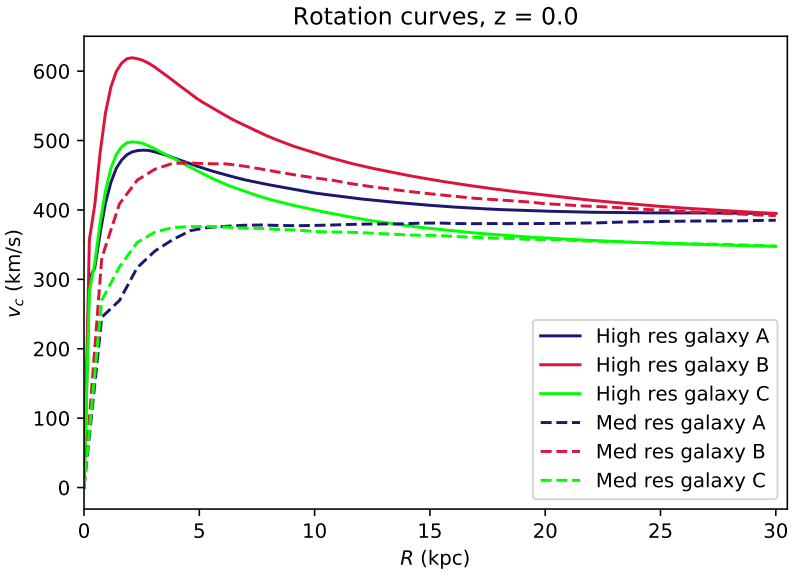

Figure 5.1: Rotation curves for each galaxy including baryons, at redshift 0. The continuous lines represent the high resolution simulations and the dasheld lines represent the medium resolution simulations.

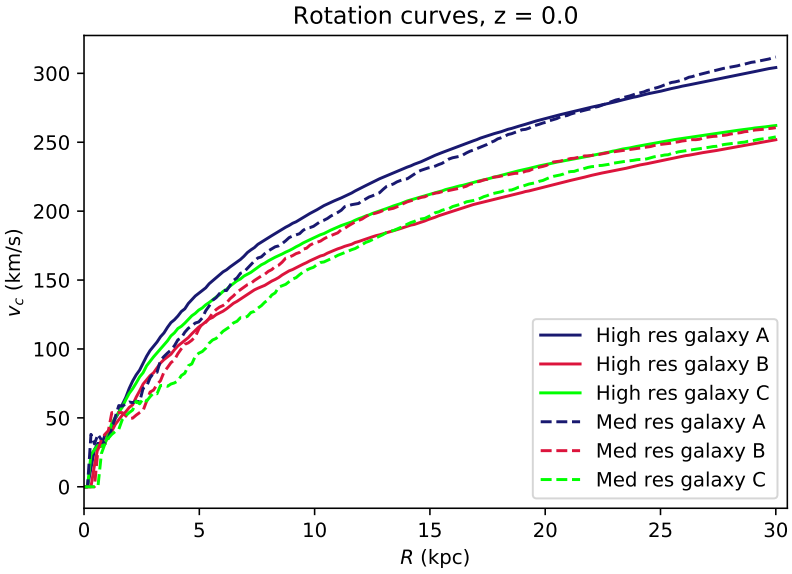

Figure 5.2: Rotation curves for each galaxy including only dark matter, at redshift 0. The continuous lines represent the high resolution simulations and the dasheld lines represent the medium resolution simulations.

5.3.2 Star formation history

- The stellar mass evolution plot is not yet done for high res simulations.

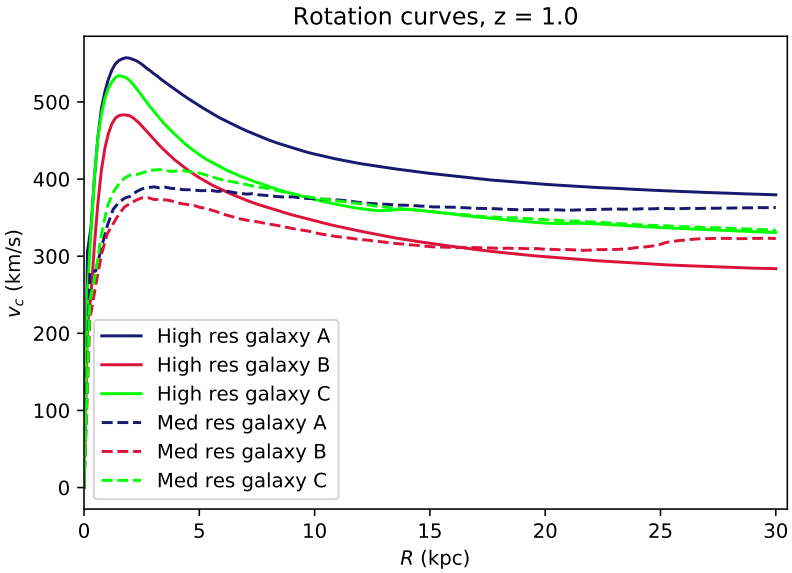

Figure 5.3: Rotation curves for each galaxy including baryons, at redshift 1. The continuous lines represent the high resolution simulations and the dasheld lines represent the medium resolution simulations.

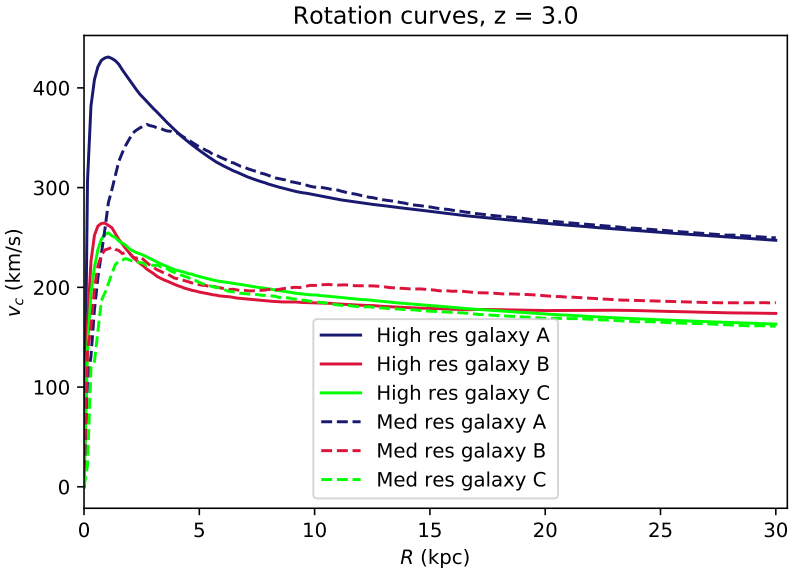

Figure 5.4: Rotation curves for each galaxy including baryons, at redshift 3. The continuous lines represent the high resolution simulations and the dasheld lines represent the medium resolution simulations.

- Redshifts missing from the stellar mass evolution plot
- SFRs, also histograms?

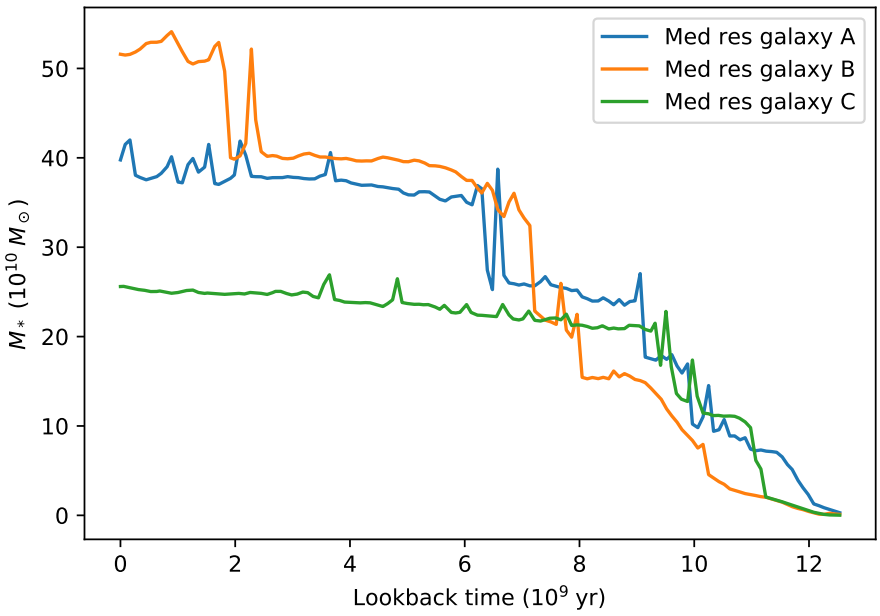

Figure 5.5: Stellar mass evolution for the medium resolution galaxies. The calculated stellar mass is the stellar mass within $r_{\mathrm{gal}} = r_{\mathrm{vir}}/10$.

- Again, med res A results will probably change a bit when double precision run is finished.
- Formation efficiencies, comparing to the cosmological parameter

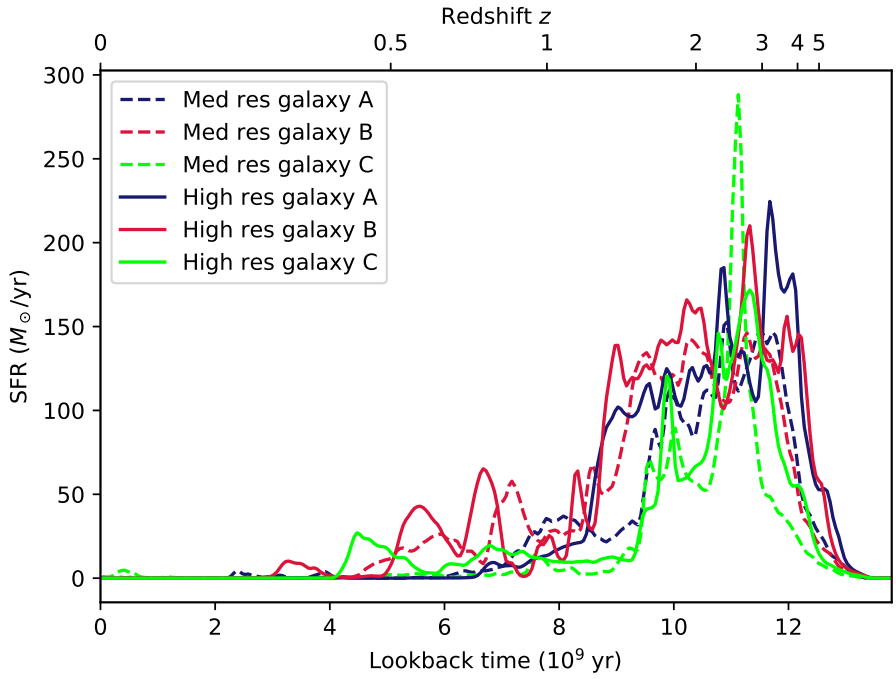

Figure 5.6: Stellar for mation rates for each zoomed-in galaxy, plottes ad a function of lookback time. The lines are created from histograms having a length of 5 Myr, which are then smoothed. The continuous lines represent the high resolution simulations and the dasheld lines represent the medium resolution simulations.

5.3.3 Colors and magnitudes

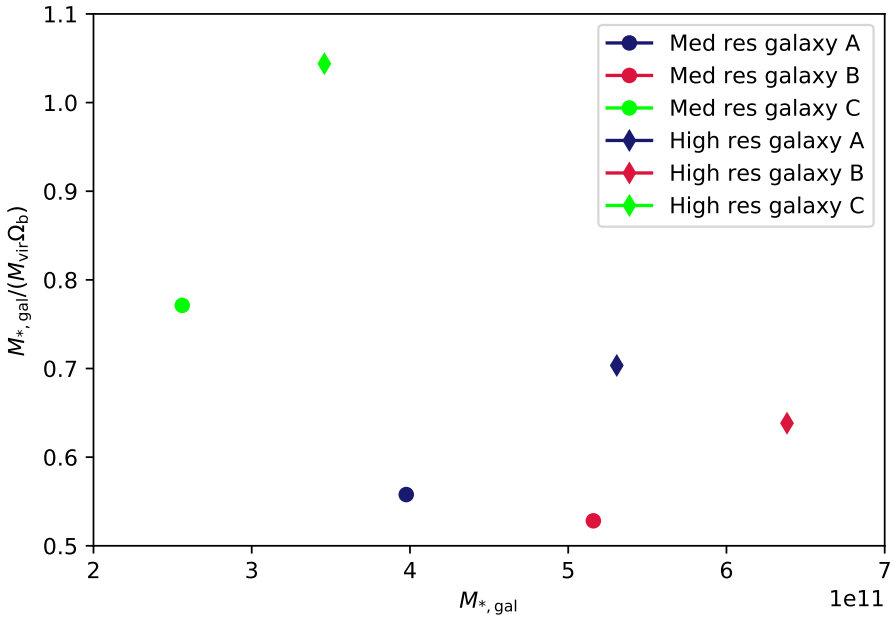

Figure 5.7: Galaxy formation efficiencies for each galaxy, plotted with their stellar masses. The cosmological baryon density Ω_{b} is set to 0.045 in the simulations. The diamond and circular markers show the results of the high resolution and the medium resolution zoom-in simulations, respectively.

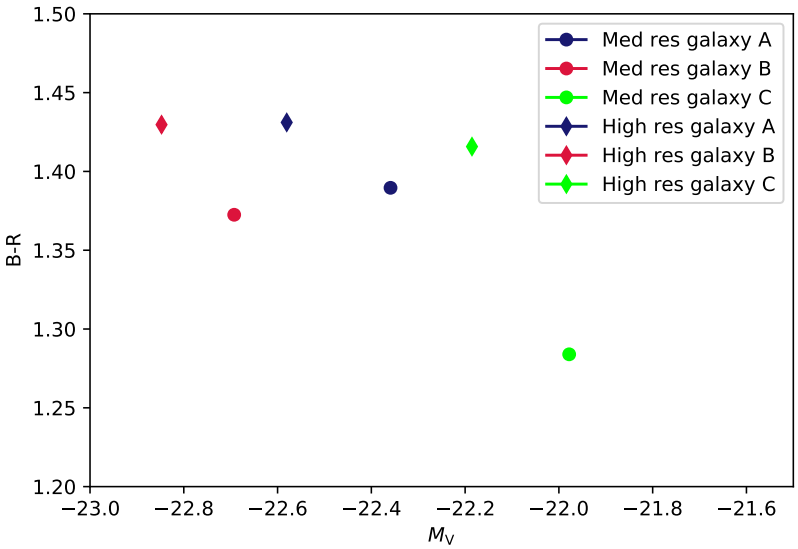

Figure 5.8: B-R colors for each simulated galaxy, plotted with each galaxy's absolute magnitude in the V-band. The diamond and circular markers show the results of the high resolution and the medium resolution zoom-in simulations, respectively.

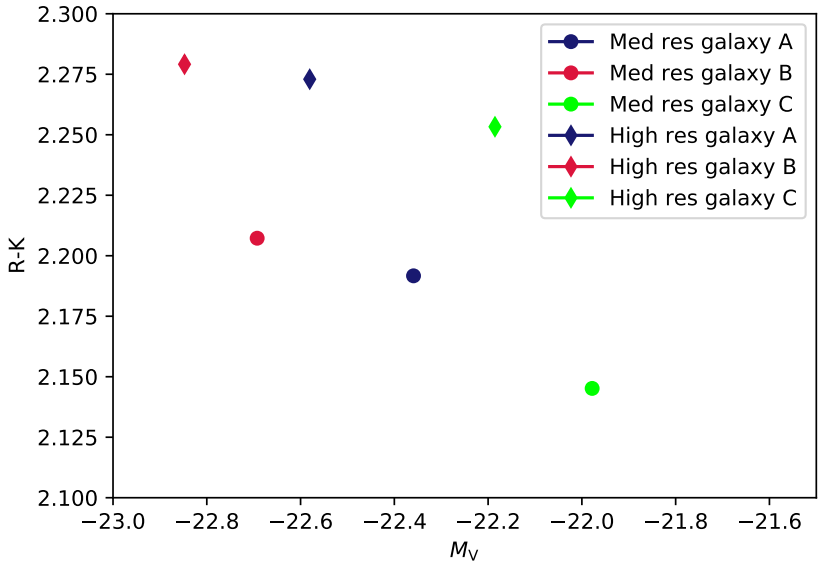

Figure 5.9: R-K colors for each simulated galaxy, plotted with each galaxy's absolute magnitude in the V-band. The diamond and circular markers show the results of the high resolution and the medium resolution zoom-in simulations, respectively.

6. Simulations with KETJU

7. Conclusions

- recap on what was written/studied
- more own thoughts on results
- future missions
- how could the simulations be more realistic (higher resolution, more feedback stuff?)

Bibliography

Bertschinger, E. (2001). Multiscale Gaussian Random Fields and Their Application to Cosmological Simulations. *The Astrophysical Journal Supplement Series*, 137(1):1–20.

Hahn, O. & Abel, T. (2011). Multi-scale initial conditions for cosmological simulations. *Monthly Notices of the Royal Astronomical Society*, 415(3):2101–2121.

Klypin, A., Kravtsov, A. V., Bullock, J. S., & Primack, J. R. (2001). Resolving the structure of cold dark matter halos. *The Astrophysical Journal*, 554(2):903–915.

Marinacci, F., Pakmor, R., & Springel, V. (2014). The formation of disc galaxies in high-resolution moving-mesh cosmological simulations. *Monthly Notices of the Royal Astronomical Soviety*, 437(2):1750–1775.

Navarro, J. F. & White, S. D. M. (1994). Simulations of dissipative galaxy formation in hierarchically clustering universes-2. Dynamics of the baryonic component in galactic haloes. *Monthly Notices of the Royal Astronomical Society*, 267(2):401–412.

Power, C., Navarro, J. F., Jenkins, A., Frenk, C. S., White, S. D. M., Springel, V., Stadel, J., & Quinn, T. (2003). The inner structure of ΛCDM haloes - I. A numerical convergence study. *Monthly Notices of the Royal Astronomical Society*, 338(1):14–34.

Reed, D. S., Smith, R. E., Potter, D., Schneider, A., Stadel, J., & Moore, B. (2013). Towards an accurate mass function for precision cosmology. *Monthly Notices of the Royal Astronomical Society*, 431(2):1866–1882.